

Effects of Palmitate on Ca^{2+} Handling in Adult Control and *ob/ob* Cardiomyocytes

Impact of Mitochondrial Reactive Oxygen Species

Jérémy Fauconnier,¹ Daniel C. Andersson,¹ Shi-Jin Zhang,¹ Johanna T. Lanner,¹ Rolf Wibom,² Abram Katz,¹ Joseph D. Bruton,¹ and Håkan Westerblad¹

Obesity and insulin resistance are associated with enhanced fatty acid utilization, which may play a central role in diabetic cardiomyopathy. We now assess the effect of the saturated fatty acid palmitate (1.2 mmol/l) on Ca^{2+} handling, cell shortening, and mitochondrial production of reactive oxygen species (ROS) in freshly isolated ventricular cardiomyocytes from normal (wild-type) and obese, insulin-resistant *ob/ob* mice. Cardiomyocytes were electrically stimulated at 1 Hz, and the signal of fluorescent indicators was measured with confocal microscopy. Palmitate decreased the amplitude of cytosolic Ca^{2+} transients (measured with fluo-3), the sarcoplasmic reticulum Ca^{2+} load, and cell shortening by ~20% in wild-type cardiomyocytes; these decreases were prevented by the general antioxidant *N*-acetylcysteine. In contrast, palmitate accelerated Ca^{2+} transients and increased cell shortening in *ob/ob* cardiomyocytes. Application of palmitate rapidly dissipated the mitochondrial membrane potential (measured with tetra-methyl rhodamine-ethyl ester) and increased the mitochondrial ROS production (measured with MitoSOX Red) in wild-type but not in *ob/ob* cardiomyocytes. In conclusion, increased saturated fatty acid levels impair cellular Ca^{2+} handling and contraction in a ROS-dependent manner in normal cardiomyocytes. Conversely, high fatty acid levels may be vital to sustain cardiac Ca^{2+} handling and contraction in obesity and insulin-resistant conditions. *Diabetes* 56:1136–1142, 2007

Cardiac muscle cells generate ATP at a high rate to support the continuous contractile function of the beating heart. Cardiac cells use various substrates to generate ATP, and the extent of substrates utilized depends on the substrate availability, the energy demand, and the physiological or pathological

condition (1). In humans as well as in different animal models, obesity, insulin resistance, and type 2 diabetes are associated with an altered cardiac metabolism characterized by an enhanced reliance on fatty acids and a decreased glucose utilization. These changes play a central role in the development of diabetic cardiomyopathy (2). For instance, application of the saturated fatty acid palmitate had markedly different effects on power output and oxygen consumption in hearts of control mice and *ob/ob* mice, which are obese, insulin resistant, and have increased serum free fatty acid concentrations (3). Moreover, *ob/ob* hearts displayed a decreased mitochondrial oxidative capacity and an increased fatty acid-induced mitochondrial uncoupling (4).

Cellular Ca^{2+} handling is altered in type 2 diabetes (5), and diabetic cardiomyopathy is characterized by defective sarcoplasmic reticulum (SR) function, which results in smaller and slower cytoplasmic Ca^{2+} transients (6,7). Mitochondria play a central role in the development of diabetes complications, and the mitochondrial dysfunction is characterized by decreased mitochondrial Ca^{2+} loading capacity and increased production of reactive oxygen species (ROS) (8–10). Increased ROS production may alter cellular Ca^{2+} handling by interfering with a wide range of proteins implicated in excitation-contraction coupling (ECC) (e.g., the SR Ca^{2+} release channels [the ryanodine receptors], the SR Ca^{2+} pumps, and the sarcolemmal $\text{Na}^+/\text{Ca}^{2+}$ exchanger [11–13]). In a recent study (14), we showed an impaired mitochondrial Ca^{2+} uptake in ventricular cardiomyocytes of *ob/ob* mice that was associated with deleterious effects on global cellular Ca^{2+} homeostasis.

In the present study, we used isolated ventricular cardiomyocytes of normal and *ob/ob* mice. The specific aims were 1) to characterize palmitate-induced changes in intracellular Ca^{2+} homeostasis and contraction and 2) to study the role of mitochondrial ROS production in these changes. The results show that palmitate has adverse, ROS-mediated effects in wild-type cardiomyocytes, whereas it improves the function of *ob/ob* cells.

RESEARCH DESIGN AND METHODS

Fluo-3 AM, tetra-methyl rhodamine-ethyl ester (TMRE), and MitoSOX Red were from Molecular Probes/Invitrogen. Carbonyl cyanide 4-(trifluoromethoxy)phenylhydrazone (FCCP), *N*-acetylcysteine (NAC), ebselen, palmitate, and laminin were from Sigma. All compounds were prepared as stock solutions in appropriate solvents. On the day of the experiment, stock solutions were diluted to the desired final concentration in the bath solution;

From the ¹Department of Physiology and Pharmacology, Karolinska Institutet, Stockholm, Sweden; and the ²Department of Laboratory Medicine, Karolinska Institutet, Stockholm, Sweden.

Address correspondence and reprint requests to Håkan Westerblad, Department of Physiology and Pharmacology, Karolinska Institutet, SE-171 77 Stockholm, Sweden. E-mail: hakan.westerblad@ki.se.

Received for publication 30 May 2006 and accepted in revised form 2 January 2007.

Published ahead of print at <http://diabetes.diabetesjournals.org> on 17 January 2007. DOI: 10.2337/db06-0739.

ECC, excitation-contraction coupling; FCCP, carbonyl cyanide 4-(trifluoromethoxy)phenylhydrazone; NAC, *N*-acetylcysteine; ROS, reactive oxygen species; SOD, superoxide dismutase; SR, sarcoplasmic reticulum; TMRE, tetra-methyl rhodamine-ethyl ester.

© 2007 by the American Diabetes Association.

The costs of publication of this article were defrayed in part by the payment of page charges. This article must therefore be hereby marked "advertisement" in accordance with 18 U.S.C. Section 1734 solely to indicate this fact.

when required, the same concentration of solvent was added to the control solution.

Animal model and cell isolation and stimulation. We used young (aged 3–5 months) C57BL leptin-deficient, obese male mice (*ob/ob*) and their wild-type counterparts (Taconic, Lille Skensved, Denmark). We recently measured body weights of ~50 and 27 g, respectively, in *ob/ob* and wild-type mice of this age range (14). Mice were killed by rapid neck disarticulation, and the heart was excised. All experiments were approved by the Stockholm North local ethical committee. Single cardiomyocytes were isolated from the ventricles following the protocols developed by the Alliance for Cellular Signaling (AfCS Procedure Protocol ID PP00000 125) (15). After being loaded with fluorescent indicators (see below), cardiomyocytes were put on laminin-coated coverslips that made up the bottom of the perfusion chamber. Cells were allowed to attach to the coverslip for ~5 min before the experiment started. They were then superfused with standard Tyrode solution (in mmol/l): 121 NaCl, 5.0 KCl, 1.8 CaCl₂, 0.5 MgCl₂, 0.4 NaH₂PO₄, 24 NaHCO₃, 0.1 EDTA, and 5.5 glucose. Palmitate (1.2 mmol/l), bound to 0.06% BSA (3), was added in some experiments. This palmitate concentration is similar to the serum concentration of fed control mice and postabsorptive *ob/ob* mice (3). The Tyrode solution was bubbled with 5% CO₂/95% O₂, which gives a bath pH of 7.4, and experiments were performed at room temperature (~24°C). Cells were continuously stimulated at 1 Hz with 1-ms current pulses delivered via two platinum electrodes, one on each side of the perfusion chamber. Measurements were only performed on rod-shaped cells that displayed a uniform contraction in response to each stimulation pulse and showed no spontaneous activity.

Measurement of cytosolic Ca²⁺ and cell shortening. The free cytosolic [Ca²⁺] was measured with the fluorescent Ca²⁺ indicator fluo-3 and confocal microscopy using a Bio-Rad MRC 1024 unit attached to a Nikon Diaphot inverted microscope with a Nikon Plan Apo 60× oil immersion objective (NA 1.3) (14). Confocal images were obtained by line scanning along the long axis, with focus in the middle of the cell. Stored confocal images were analyzed with ImageJ (National Institutes of Health [available at <http://rsb.info.nih.gov/ij/>]). To enable comparisons between cells, changes in the fluo-3 fluorescence signal (ΔF) were divided by the fluorescence immediately before a stimulation pulse was given under control conditions (F_0). The time course of Ca²⁺ transients was assessed by measuring the half-width ($D_{1/2}$ [i.e., the duration at 50% of ΔF]) and the time constant (τ) of the exponential part of the decay phase, ignoring the initial phase that often diverges from a monoexponential function. The edges of the fluorescence images of the cells were followed during contractions, which allowed determination of cell shortening simultaneously with measurements of Ca²⁺. The cell length was measured in the rested state and the maximally contracted state, and shortening is expressed as a percentage of the resting cell length. Measurements of Ca²⁺ transients and cell shortening were performed immediately before and 20 min after palmitate exposure.

Measurements of mitochondrial membrane potential. TMRE was used to measure mitochondrial membrane potential ($\Delta\Psi_m$) (16). Isolated cardiomyocytes were loaded with TMRE (1 μ mol/l) in Dulbecco's modified Eagle's medium for 15 min at room temperature, followed by washout in medium without TMRE. Confocal images of TMRE fluorescence were obtained by excitation at 568 nm while measuring the emitted light at 585 nm. To minimize the impact of subcellular variability in $\Delta\Psi_m$, TMRE fluorescence was measured in five different areas in each cell (16). Images were taken every 5 min, and fluorescence signals were normalized to the fluorescence measured in each cell at the start of the experiment, which was set to 100%. At the end of each experiment, cells were exposed to the mitochondrial uncoupler FCCP (1 μ mol/l) to determine the dynamic range of the dye.

Measurements of mitochondrial ROS production. MitoSOX Red was used to measure mitochondrial ROS production (17). Isolated cardiomyocytes were loaded with MitoSOX Red (5 μ mol/l) in Dulbecco's modified Eagle's medium for 15 min at room temperature, followed by washout. Confocal images were obtained at 5-min intervals by excitation at 488 nm and measuring the emitted light at 585 nm. MitoSOX Red fluorescence was measured at each time point as the mean of five measurements performed at different areas in each cell. The signal from each cell was normalized to that at the start of the experiment, which was set to 100%. As a positive control, 1 mmol/l of H₂O₂ was added at the end of each experiment, and this resulted in a marked increase in the fluorescence signal in all cells (data not shown).

Measurements of aconitase activity. Immediately after killing the mouse, the heart was excised and the ventricles were dissected and frozen in liquid nitrogen. The ventricles were homogenized (50 μ l/mg wet wt) with ground-glass homogenizers in ice-cold buffer consisting of (in mmol/l): 50 Tris-HCl, 5 sodium citrate, 0.6 MnCl₂, 1 cysteine, and 0.05% (vol/vol) Triton X-100 (pH 7.4). The homogenate was centrifuged at 4°C at 1,400g for 1 min, and an aliquot of the supernatant immediately was assayed for aconitase activity following the conversion of citrate to isocitrate coupled with isocitrate dehydrogenase

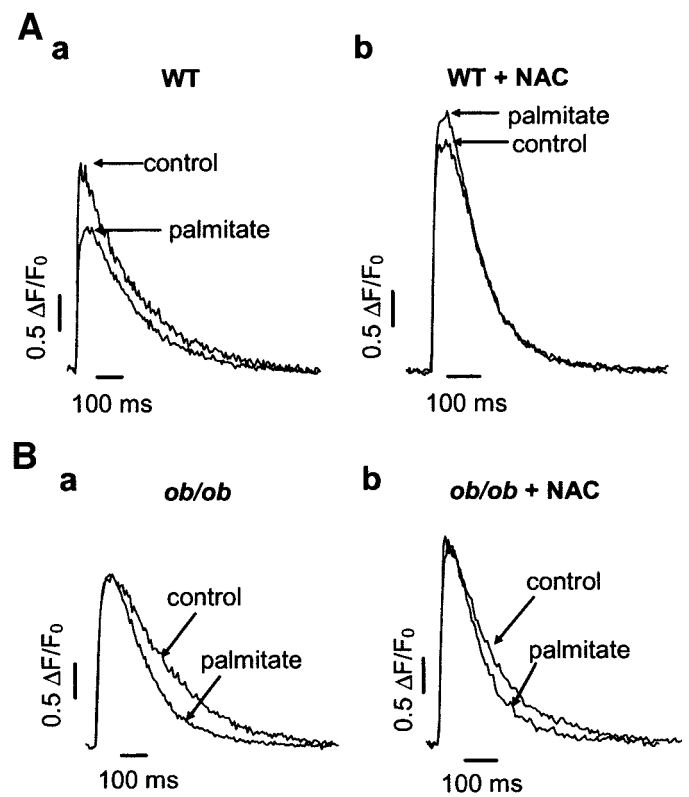


FIG. 1. Representative spatially averaged Ca²⁺ transients (expressed as normalized fluo-3 fluorescence) from a wild-type (WT) (A) and an *ob/ob* (B) cardiomyocyte. Transients were obtained in the absence (a) and presence (b) of NAC (20 mmol/l) and during exposure to palmitate (1.2 mmol/l) as indicated.

(measuring the production of NADPH at 340 nm) (18). The remaining supernatant was stored at -80°C until assayed for citrate synthase activity (19) and protein (Bio-Rad). The protein concentration was not different between wild-type and *ob/ob* hearts (88.1 ± 0.7 vs. 87.4 ± 2.4 μ g/mg wet wt; $n = 4$). The enzyme activities of each heart were corrected for protein concentration.

Western blot analyses. Frozen ventricles were homogenized in lysis buffer consisting of 50 mmol/l KH₂PO₄ (pH 7.5), 1 mmol/l EDTA, 0.05% Triton X-100 (vol/vol), and protease inhibitor cocktail (Roche). Lysates were cleared by centrifugation at 1,400g for 30 s at 4°C. The protein content was determined using the Bradford assay (Bio-Rad). Equal amounts of total protein (30 μ g) were loaded into each well and separated by electrophoresis using NuPAGE Novex 4–12% Bis-Tris Gels (Invitrogen) and transferred onto a polyvinylidene fluoride membrane (Bio-Rad). Membranes were blocked in 5% (wt/vol) nonfat milk in Tris-buffered saline containing 0.05% Tween 20, followed by incubation with primary antibody (anti-SOD2, Biosite; 1:1,000 dilution). Membranes then were incubated with horseradish peroxidase-conjugated antibody (anti-goat Ig; 1:2,000 dilution), and immunoreactive bands were visualized using chemiluminescence (Super Signal; Pierce). Membranes then were stripped and rebotted against the dihydropyridine receptor (anti-DHPR, Abcam; 1:500 dilution), which served as a loading control, followed by incubation with horseradish peroxidase-conjugated antibody (anti-mouse Ig; 1:1,000 dilution).

Statistics. Data are presented as means ± SE, and the number of cardiomyocytes (n) is given. For each experimental condition, cells were isolated from at least three age-matched mice, except in the ebselen experiments, where only two mice were used in each condition. Statistically significant differences were assessed with Student's *t* test (for paired or unpaired samples) or, when three or more groups were compared, one-way ANOVA with a Newman-Keuls post hoc test. $P < 0.05$ was considered significant.

RESULTS

Effects of palmitate on cytosolic Ca²⁺ transients, contraction, and SR Ca²⁺ load. Under control conditions, Ca²⁺ transients were smaller and slower in *ob/ob* compared with wild-type cardiomyocytes (Fig. 1; Table 1)

TABLE 1
Ca²⁺ transient characteristics in the presence or absence of 1.2 mmol/l palmitate

	<i>n</i>	$\Delta F/F_0$	$D_{1/2}$ (ms)	τ (ms)
Wild-type mice				
Control	28	3.2 ± 0.1	188.5 ± 5.7	184.8 ± 8.4
Palmitate	30	2.6 ± 0.1*	206.1 ± 4.6*	214.1 ± 7.2*
<i>ob/ob</i> mice				
Control	30	2.7 ± 0.1†	232.4 ± 7.8†	211.1 ± 6.3†
Palmitate	27	3.0 ± 0.1	211.0 ± 7.9*	187.0 ± 7.8*†

Data are means ± SE. **P* < 0.05 vs. the basal condition within each group (wild-type or *ob/ob*). †*P* < 0.05 *ob/ob* vs. wild-type when studied under the same conditions. $\Delta F/F_0$, peak amplitude; τ , decay time constant; $D_{1/2}$, half-width.

(14). In wild-type cells, application of palmitate significantly decreased the Ca²⁺ transient amplitude by ~20% and increased half-width as well as the decay time constant (Table 1). In *ob/ob* cardiomyocytes, on the other hand, palmitate did not have any significant effect on the Ca²⁺ transient amplitude, but the transients became significantly faster (Fig. 1; Table 1).

In the presence of palmitate, relative cell shortening was decreased by ~20% in wild-type cardiomyocytes (Fig. 2Aa), whereas it was increased by ~40% in *ob/ob* cells (Fig.

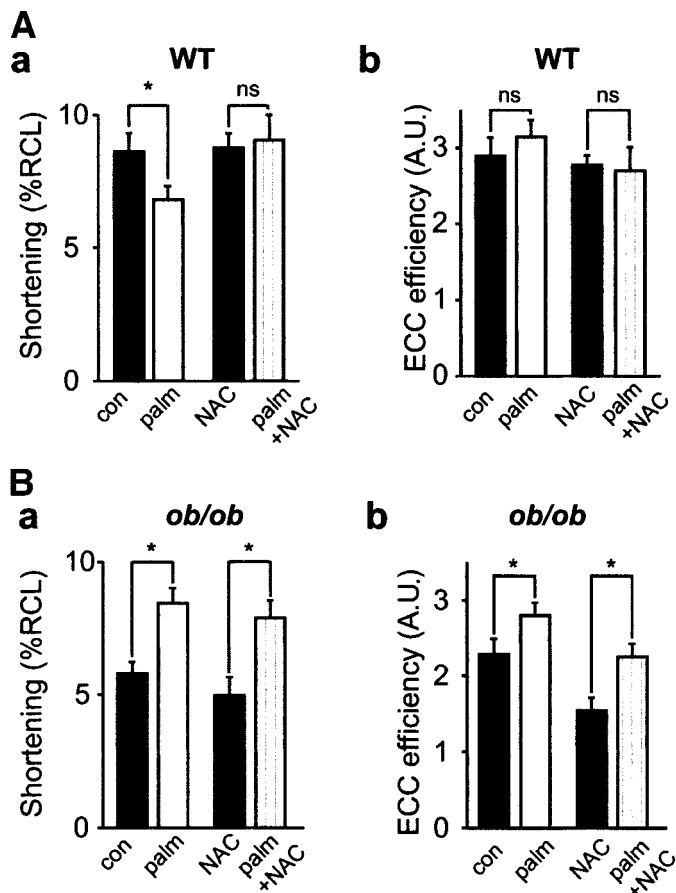


FIG. 2. Palmitate improved contractile function of *ob/ob* cardiomyocytes. Mean data (± SE; *n* = 10–16 cells) of cell shortening (a) and ECC efficiency (b) in wild-type (WT) (A) and *ob/ob* (B) cells. Cell shortening is as a percentage of the resting cell length (RCL) and ECC efficiency is the ratio between the relative cell shortening and the Ca²⁺ transient amplitude. NAC (20 mmol/l) and palmitate (1.2 mmol/l) exposure as indicated. *Statistical difference between the absence and presence of palmitate (*P* < 0.05).

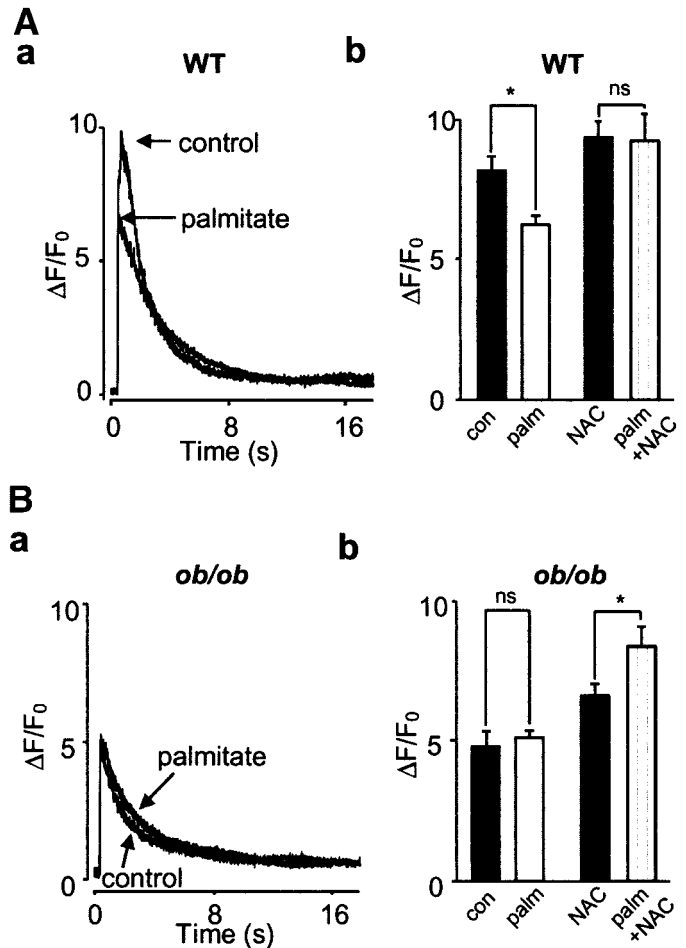


FIG. 3. Palmitate decreased the SR Ca²⁺ content in wild-type cardiomyocytes. Representative spatially averaged Ca²⁺ transients induced by application of caffeine (10 mmol/l) in a wild-type (WT) (Aa) and an *ob/ob* (Ba) cardiomyocyte in the absence and presence of palmitate (1.2 mmol/l) as indicated. Mean data (± SE; *n* = 8–12 cells) from wild-type (Ab) and *ob/ob* (Bb) cells. NAC (20 mmol/l) and palmitate exposure is indicated below the bars. *Statistical difference between the absence and presence of palmitate (*P* < 0.05).

2Ba). Palmitate significantly increased the ECC efficiency (i.e., the ratio between the relative cell shortening and the amplitude of the Ca²⁺ transient) by ~25% in *ob/ob* cells (Fig. 2Bb). In wild-type cardiomyocytes, on the other hand, palmitate had no significance in the ECC efficiency (Fig. 2Ab) due to the concomitant decreases in cell shortening and Ca²⁺ transient amplitude.

The SR Ca²⁺ content was assessed by measuring the amplitude of cytosolic Ca²⁺ transients induced by rapid application of caffeine (20). In these experiments, the steady-state Ca²⁺ transients were established during 25-min continuous stimulation in the absence or presence of palmitate. The stimulation was then stopped and the superfusate was rapidly switched to a solution containing caffeine (10 mmol/l). In the presence of palmitate, the amplitude of the caffeine-induced Ca²⁺ transient was decreased by ~25% in wild-type cardiomyocytes (Fig. 3A), whereas it was not affected in *ob/ob* cells (Fig. 3B). To sum up, in wild-type cells, palmitate decreased the amplitude of electrically evoked Ca²⁺ transients and the SR Ca²⁺ content, and this led to a reduced cell shortening. In *ob/ob* cardiomyocytes, on the other hand, palmitate made the Ca²⁺ transient faster without affecting the SR Ca²⁺ content and cell shortening was enhanced.

The antioxidants NAC and ebselen prevent the palmitate-induced impairment in wild-type cardiomyocyte function. Increased mitochondrial ROS production and oxidative stress are known to affect Ca^{2+} handling in cardiac cells (12,13). Therefore, we hypothesized that the impaired cellular Ca^{2+} handling induced by palmitate in wild-type cells was caused by increased mitochondrial ROS production. To test this hypothesis, we measured cytosolic Ca^{2+} transients and cell shortening in the presence of the nonspecific antioxidant NAC (20 mmol/l). In wild-type cardiomyocytes, palmitate application in the presence of NAC did not affect the Ca^{2+} transient characteristics (Fig. 1Ab; Table 2), the cell shortening or the ECC efficiency (Fig. 2A), or the SR Ca^{2+} content (Fig. 3A). In *ob/ob* cardiomyocytes, on the other hand, NAC had no effect on the palmitate-induced increases in Ca^{2+} transient kinetics, shortening amplitude, and ECC efficiency (Figs. 1Bb and 2B; Table 2), whereas it increased the SR Ca^{2+} content (Fig. 3B).

We also studied Ca^{2+} transients in the presence of another antioxidant, ebselen (5 $\mu\text{mol/l}$), which acts as a glutathione peroxidase mimetic that removes hydrogen peroxide in the presence of reduced glutathione (21). The effects of ebselen were similar to those obtained with NAC (Table 2). Thus, in the presence of ebselen, palmitate had no effect on Ca^{2+} transient characteristics in wild-type cells, whereas palmitate still made the Ca^{2+} transients faster in *ob/ob* cells (although the decrease in τ did not reach statistical significance). In summary, these results with antioxidants indicate that the palmitate-induced changes in cellular Ca^{2+} handling in wild-type cardiomyocytes were mediated by increased ROS production, whereas the palmitate effects in *ob/ob* cells mostly were ROS independent.

Effects of palmitate on mitochondrial membrane potential ($\Delta\Psi_m$) and ROS production. Application of palmitate resulted in a highly significant decrease in the TMRE fluorescence within 5 min in wild-type cardiomyocytes, whereas there was no change in *ob/ob* cells over the 25-min observation period (Fig. 4). Addition of FCCP (1 $\mu\text{mol/l}$), a mitochondrial uncoupler that dissipates $\Delta\Psi_m$, resulted in a prompt decrease of the TMRE fluorescence in both wild-type and *ob/ob* cardiomyocytes. After 5 min exposure to FCCP, the TMRE signal was similar in wild-type and *ob/ob* cells (Fig. 4A).

We next tested the effect of palmitate on mitochondrial ROS production using MitoSOX Red, which is targeted to

TABLE 2
 Ca^{2+} transient characteristics in the presence of NAC or ebselen with or without 1.2 mmol/l palmitate

	<i>n</i>	$\Delta F/F_0$	$D_{1/2}$ (ms)	τ (ms)
Wild-type mice				
NAC	12	3.8 ± 0.2	165.1 ± 5.1	154.7 ± 4.9
NAC + palmitate	12	3.4 ± 0.2	177.5 ± 4.9	149.5 ± 4.3
Ebselen	14	3.3 ± 0.3	174.1 ± 3.5	167.1 ± 7.5
Ebselen + palmitate	14	3.4 ± 0.3	180.7 ± 5.9	170.2 ± 10.3
<i>ob/ob</i> mice				
NAC	15	3.2 ± 0.1	154.8 ± 4.2	158.4 ± 11.5
NAC + palmitate	15	3.5 ± 0.3	$138.5 \pm 3.1^*$	$131.7 \pm 4.6^*$
Ebselen	15	3.1 ± 0.2	218.7 ± 8.3	201.7 ± 9.4
Ebselen + palmitate	16	3.4 ± 0.2	$189.3 \pm 6.4^*$	183.6 ± 7.0

Data are means \pm SE. * $P < 0.05$, palmitate vs. no palmitate within each group (wild-type or *ob/ob*). $\Delta F/F_0$, peak amplitude; τ , decay time constant; $D_{1/2}$, half-width.

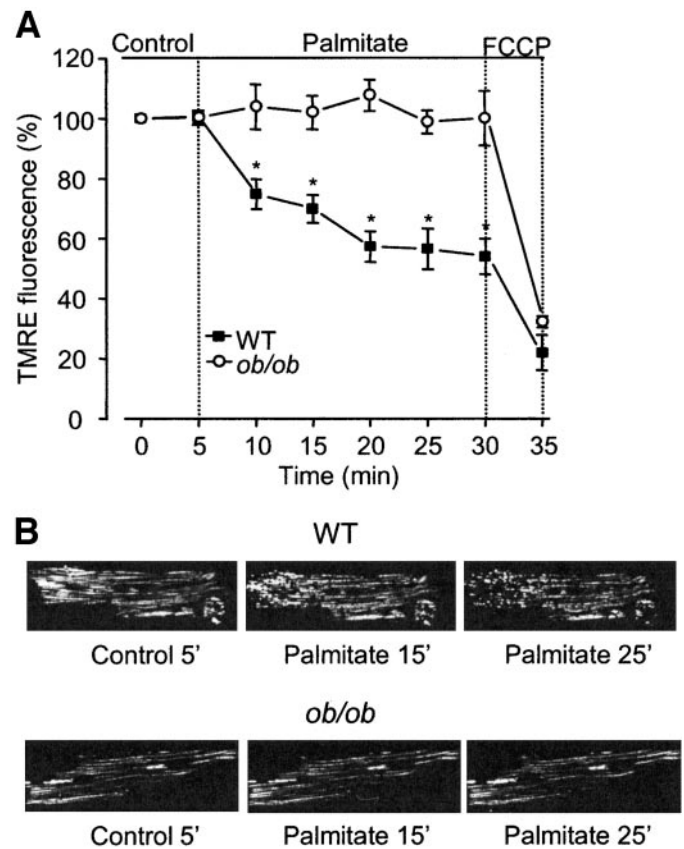


FIG. 4. Palmitate dissipated $\Delta\Psi_m$ in wild-type but not in *ob/ob* cardiomyocytes. **A:** The normalized TMRE fluorescence recorded under control conditions, during 25 min with 1.2 mmol/l palmitate, and finally after 5 min in 1 $\mu\text{mol/l}$ FCCP. Data are means \pm SE from 16 to 25 cells; ■, wild-type (WT); ○, *ob/ob*. *Statistical difference between the two groups ($P < 0.05$). **B:** Typical images of a wild-type (WT) (upper row) and an *ob/ob* (lower row) cell. Images were obtained after 5 min under control conditions and after 15 and 25 min in the presence of palmitate. Note the marked palmitate-induced decrease in fluorescent light (reflecting a decreased $\Delta\Psi_m$) in the wild-type cell.

the mitochondria and increases its fluorescence when oxidized. Palmitate application caused a rapid increase in the MitoSOX Red signal in wild-type cardiomyocytes but not in *ob/ob* cardiomyocytes (Fig. 5). Thus, these results show that palmitate exposure induced a marked depolarization of $\Delta\Psi_m$ and increased the mitochondrial ROS production in wild-type but not in *ob/ob* cardiomyocytes.

Estimates of mitochondrial ROS production in vivo. While MitoSOX Red readily detects changes in mitochondrial ROS production during an experiment, it is less suitable for detecting differences in basal mitochondrial ROS production between different cell populations. This is because it is a nonratiometric indicator, and, hence, the basal fluorescence depends on, for instance, the concentration of the dye. Thus, the MitoSOX Red results presented in Fig. 5 do not provide any information regarding possible differences in mitochondrial ROS production in wild-type and *ob/ob* hearts. One way to assess this is to measure the aconitase activity because the function of this mitochondrial enzyme critically depends on an iron-sulfur cluster, and proteins with such clusters may lose activity in response to increased mitochondrial oxidative stress (18). The aconitase activity was similar in wild-type and *ob/ob* hearts (Fig. 6A). We also measured the citrate synthase activity, which is frequently used to assess the cellular mitochondrial content, and found no difference

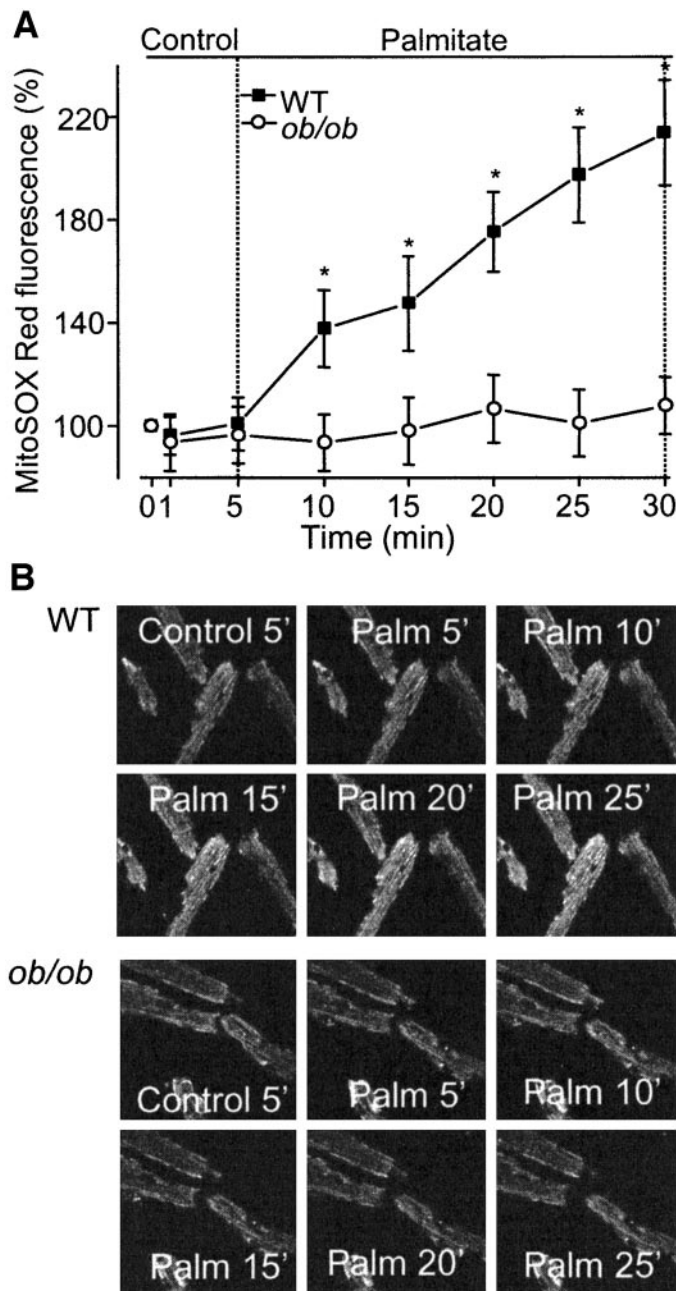


FIG. 5. Palmitate increased the mitochondrial ROS production in wild-type but not in *ob/ob* cardiomyocytes. **A:** The normalized MitoSOX Red fluorescence recorded under control conditions and during 25 min with palmitate. Data are means \pm SE from 10 cells in each group. ■, wild-type (WT); ○, *ob/ob*. *Statistical difference between the two groups ($P < 0.05$). **B:** Typical images of wild-type (WT) (*upper panel*) and *ob/ob* (*lower panel*) cells. Images obtained after 5 min under control conditions and at 5-min intervals in the presence of palmitate. Note the marked palmitate-induced increase in fluorescent light (reflecting increased ROS) in the wild-type cells.

between wild-type and *ob/ob* hearts (127 ± 3 vs. 131 ± 3 $\mu\text{mol} \cdot \text{min}^{-1} \cdot \text{g}^{-1}$ wet wt; $n = 4$).

Mitochondrial manganese-dependent superoxide dismutase (MnSOD or SOD2) plays a central role in the defense against superoxide ions produced by respiration. The expression of SOD2 generally is upregulated in response to an increased mitochondrial ROS production (22). We used Western blots to measure SOD2 protein expression and found no difference between *ob/ob* and wild-type hearts (Fig. 6B).

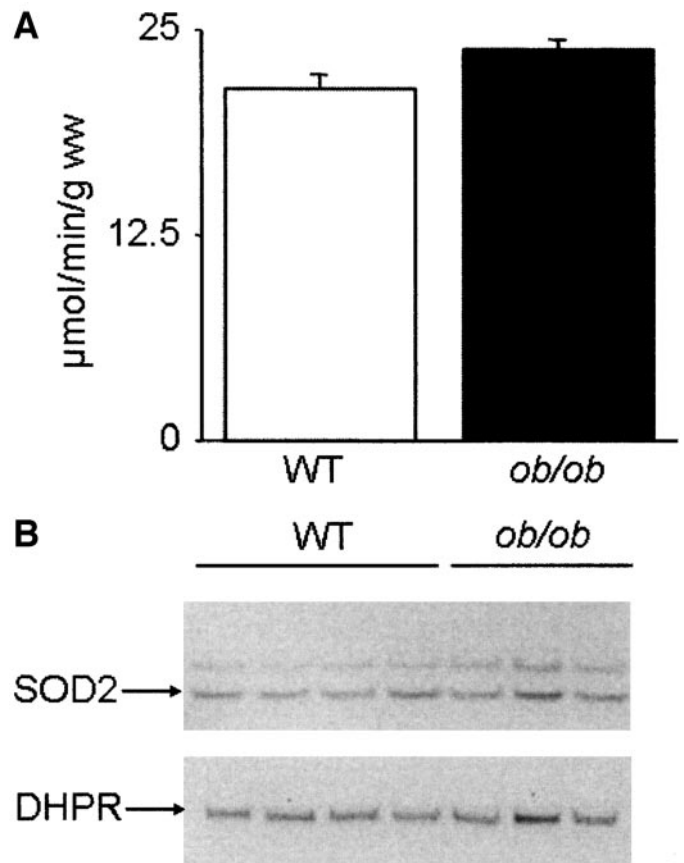


FIG. 6. No difference in aconitase activity or SOD2 expression between wild-type and *ob/ob* hearts. **A:** Mean data (\pm SE; $n = 4$) of aconitase activity in wild-type (WT) (■) and *ob/ob* (□) hearts. **B:** SOD2 and dihydropyridine receptor (DHPR) immunoblots of wild-type (WT) and *ob/ob* hearts as indicated. Note that the expression of SOD2 was similar in the two groups. A total of 30 μg total protein was loaded into each well, and DHPR was used as a control for equal loading.

Palmitate supply prevents Ca²⁺ alternans in *ob/ob*. Inhibition of glycolysis and altered glucose oxidation may cause Ca²⁺ alternans, which is defined as Ca²⁺ transients of alternating amplitude on a beat-to-beat basis (23–25). In the normal Tyrode solution, no wild-type cells displayed Ca²⁺ alternans, whereas it was present in 19% of the *ob/ob* cells, i.e., 7 of 37 cells. (These cells were not included in the Ca²⁺ transient analyses described above because the amplitude and kinetics varied on a beat-to-beat basis.)

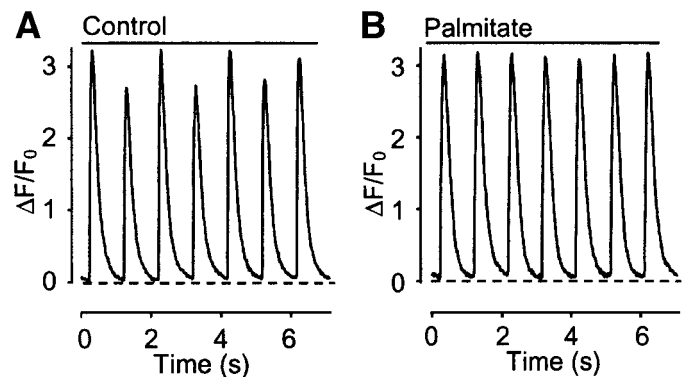


FIG. 7. Typical records of cytosolic Ca²⁺ transients in an *ob/ob* cardiomyocyte in the absence (**A**) and presence (**B**) of palmitate (1.2 mmol/l). Note that this cell displayed Ca²⁺ alternans that disappeared during palmitate exposure.

After application of palmitate, Ca^{2+} alternans were abolished in the *ob/ob* cells that displayed this behavior (Fig. 7). Thus, no Ca^{2+} alternans were observed in either wild-type or *ob/ob* cardiomyocytes in the presence of palmitate.

DISCUSSION

The heart is metabolically versatile, switching its preferred substrate depending on the environmental and physiological or pathological conditions (1). In line with this, recent studies (3,4) showed markedly different responses when hearts from wild-type and insulin-resistant *ob/ob* mice were exposed to the saturated fatty acid palmitate. The aim of the present study was to reveal cellular mechanisms underlying these differences. Our results show that application of palmitate had adverse effects in wild-type cardiomyocytes (i.e., it impaired intracellular Ca^{2+} handling and contraction, depolarized $\Delta\Psi_m$, and increased mitochondrial ROS production). In *ob/ob* cardiomyocytes, on the other hand, palmitate exposure improved cellular Ca^{2+} handling and contraction and prevented the occurrence of Ca^{2+} alternans, whereas it had no effect on $\Delta\Psi_m$ or ROS production.

Palmitate adversely affects wild-type cardiomyocyte function. Hyperglycemia and high serum free fatty acid levels are important contributors to the pathological adaptations in diabetes, and they share at least one pathogenic mechanism: overproduction of ROS by the mitochondrial electron-transport chain (26–28). Moreover, several studies (27,29–31) have demonstrated that long-chain saturated fatty acids, such as palmitate, can promote apoptosis in a variety of cell types, including adult cardiomyocytes. Palmitate-induced proapoptotic signaling has been associated with $\Delta\Psi_m$ dissipation and increased ROS production (27,29,30). The mitochondrial ROS production is likely to occur mainly at the level of complexes I and III of the mitochondrial respiratory chain, and the function of both these complexes has been shown to be altered by palmitate (29,32). Increased ROS production may impair cellular Ca^{2+} handling by decreasing the L-type Ca^{2+} current amplitude, increasing the open probability of the SR Ca^{2+} release channels, slowing SR Ca^{2+} reuptake, and increasing the sarcolemmal $\text{Na}^+/\text{Ca}^{2+}$ exchange activity, eventually leading to reduced SR Ca^{2+} content (11,33–35). Thus, the present results in wild-type cardiomyocytes all can be explained by a model in which palmitate dissipates $\Delta\Psi_m$ and increases mitochondrial ROS production (Figs. 4 and 5), which results in impaired SR Ca^{2+} handling and, consequently, decreased shortening (Figs. 1–3). In accordance with this model, palmitate had no effect on SR Ca^{2+} handling and contraction in wild-type cells in the presence of antioxidants.

Palmitate has positive effects on *ob/ob* cardiomyocyte function. In contrast to the situation in wild-type cardiomyocytes, palmitate application did not affect the $\Delta\Psi_m$ or mitochondrial ROS production in *ob/ob* cardiomyocytes. Accordingly, antioxidants had no effect on palmitate-induced changes in Ca^{2+} handling and contraction in *ob/ob* cells. Furthermore, aconitase activity and SOD2 protein expression were not significantly different between wild-type and *ob/ob* cardiomyocytes (Fig. 6), which indicates no major difference in mitochondrial ROS production in vivo between the two groups despite the fact that *ob/ob* hearts are exposed to a markedly higher concentration of saturated fatty acids (3).

A number of studies have reported an increased fatty acid oxidation associated with a marked reduction of glycolysis and glucose oxidation in obesity and type 2 diabetes (2–4,36–38). This metabolic switch suggests a faster ATP production with palmitate than with glucose in *ob/ob* cardiomyocytes. Accordingly, palmitate induced a NAC- and ebselen-independent increase in the rate of SR Ca^{2+} reuptake, the extent of cell shortening, and the ECC efficiency in *ob/ob* cells. These processes depend on ATPase activity and would be accelerated by an improved mitochondrial ATP production, resulting in an increased ATP-to-ADP ratio and decreased inorganic phosphate ion concentration (39–41). Furthermore, inhibition of energy metabolism leading to decreased ATP formation has been shown to impair SR Ca^{2+} release and reuptake (39,42,43), and this can lead to unstable Ca^{2+} cycling in a beat-to-beat basis and favor the occurrence of Ca^{2+} alternans (44). Although the exact mechanisms of Ca^{2+} alternans still is unclear, an alternating SR Ca^{2+} load seems to be a major event in triggering Ca^{2+} alternans, and faster SR Ca^{2+} uptake may stabilize the SR Ca^{2+} load and prevent Ca^{2+} alternans (25,45). Accordingly, Ca^{2+} alternans frequently were observed in *ob/ob* cells in the presence of glucose, but never after application of palmitate, where the rate of SR Ca^{2+} uptake was increased.

Conclusion. Based on the present results, we propose a model in which high fatty acid levels initially induce increased mitochondrial ROS production, which has serious negative effects on cardiomyocyte function. During prolonged exposure to increased fatty acid levels, as in *ob/ob* mice, cardiomyocytes adapt so that fatty acids are preferred to glucose as a substrate for energy metabolism, and, hence, fatty acid exposure results in improved cellular Ca^{2+} handling and contraction.

ACKNOWLEDGMENTS

The present study was supported by the Swedish Research Council (project no. 10842 and 14453), the Swedish Heart and Lung Foundation, the Swedish Diabetes Foundation, and Funds at the Karolinska Institutet.

REFERENCES

1. Stanley WC, Recchia FA, Lopaschuk GD: Myocardial substrate metabolism in the normal and failing heart. *Physiol Rev* 85:1093–1129, 2005
2. Carley AN, Severson DL: Fatty acid metabolism is enhanced in type 2 diabetic hearts. *Biochim Biophys Acta* 1734:112–126, 2005
3. Mazumder PK, O'Neill BT, Roberts MW, Buchanan J, Yun UJ, Cooksey RC, Boudina S, Abel ED: Impaired cardiac efficiency and increased fatty acid oxidation in insulin-resistant *ob/ob* mouse hearts. *Diabetes* 53:2366–2374, 2004
4. Boudina S, Sena S, O'Neill BT, Tathireddy P, Young ME, Abel ED: Reduced mitochondrial oxidative capacity and increased mitochondrial uncoupling impair myocardial energetics in obesity. *Circulation* 112:2686–2695, 2005
5. Levy J: Abnormal cell calcium homeostasis in type 2 diabetes mellitus: a new look on old disease. *Endocrine* 10:1–6, 1999
6. Fang ZY, Prins JB, Marwick TH: Diabetic cardiomyopathy: evidence, mechanisms, and therapeutic implications. *Endocr Rev* 25:543–567, 2004
7. Belke DD, Swanson EA, Dillmann WH: Decreased sarcoplasmic reticulum activity and contractility in diabetic *db/db* mouse heart. *Diabetes* 53:3201–3208, 2004
8. Flarsheim CE, Grupp IL, Matlib MA: Mitochondrial dysfunction accompanies diastolic dysfunction in diabetic rat heart. *Am J Physiol* 271:H192–H202, 1996
9. Duchen MR: Roles of mitochondria in health and disease. *Diabetes* 53 (Suppl. 1):S96–S102, 2004
10. Brownlee M: The pathobiology of diabetic complications: a unifying mechanism. *Diabetes* 54:1615–1625, 2005
11. Kourie JI: Interaction of reactive oxygen species with ion transport mechanisms. *Am J Physiol* 275:C1–C24, 1998

12. Giordano FJ: Oxygen, oxidative stress, hypoxia, and heart failure. *J Clin Invest* 115:500–508, 2005
13. Zima AV, Blatter LA: Redox regulation of cardiac calcium channels and transporters. *Cardiovasc Res* 71:310–321, 2006
14. Fauconnier J, Lanner JT, Zhang SJ, Tavi P, Bruton JD, Katz A, Westerblad H: Insulin and inositol 1,4,5-trisphosphate trigger abnormal cytosolic Ca²⁺ transients and reveal mitochondrial Ca²⁺ handling defects in cardiomyocytes of *ob/ob* mice. *Diabetes* 54:2375–2381, 2005
15. Sambrano GR, Fraser I, Han H, Ni Y, O'Connell T, Yan Z, Stull JT: Navigating the signalling network in mouse cardiac myocytes. *Nature* 420:712–714, 2002
16. Duchen MR, Leyssens A, Crompton M: Transient mitochondrial depolarizations reflect focal sarcoplasmic reticular calcium release in single rat cardiomyocytes. *J Cell Biol* 142:975–988, 1998
17. Ooe H, Taira T, Iguchi-Ariga SM, Ariga H: Induction of reactive oxygen species by bisphenol A and abrogation of bisphenol A-induced cell injury by DJ-1. *Toxicol Sci* 88:114–126, 2005
18. Gardner PR: Aconitase: sensitive target and measure of superoxide. *Methods Enzymol* 349:9–23, 2002
19. Srere PA: Citrate synthase: [EC 4.1.3.7. Citrate oxaloacetate-lyase (CoA-acetylating)]. *Methods Enzymol* 13:3–11, 1969
20. Maier LS, Zhang T, Chen L, DeSantiago J, Brown JH, Bers DM: Transgenic CaMKII δ_C overexpression uniquely alters cardiac myocyte Ca²⁺ handling: reduced SR Ca²⁺ load and activated SR Ca²⁺ release. *Circ Res* 92:904–911, 2003
21. Cotgreave IA, Sandy MS, Berggren M, Moldeus PW, Smith MT: N-acetylcysteine and glutathione-dependent protective effect of PZ51 (Ebselen) against diquat-induced cytotoxicity in isolated hepatocytes. *Biochem Pharmacol* 36:2899–2904, 1987
22. Storz P, Döppler H, Toker A: Protein kinase D mediates mitochondrion-to-nucleus signaling and detoxification from mitochondrial reactive oxygen species. *Mol Cell Biol* 25:8520–8530, 2005
23. O'Rourke B, Ramza BM, Marban E: Oscillations of membrane current and excitability driven by metabolic oscillations in heart cells. *Science* 265:962–966, 1994
24. Kockskämper J, Blatter LA: Subcellular Ca²⁺ alternans represents a novel mechanism for the generation of arrhythmogenic Ca²⁺ waves in cat atrial myocytes. *J Physiol* 545:65–79, 2002
25. Eisner DA, Diaz ME, Li Y, O'Neill SC, Trafford AW: Stability and instability of regulation of intracellular calcium. *Exp Physiol* 90:3–12, 2005
26. Unger RH, Orci L: Diseases of liporegulation: new perspective on obesity and related disorders. *FASEB J* 15:312–321, 2001
27. Listenberger LL, Schaffer JE: Mechanisms of lipoapoptosis: implications for human heart disease. *Trends Cardiovasc Med* 12:134–138, 2002
28. Ye G, Metreveli NS, Donthi RV, Xia S, Xu M, Carlson EC, Epstein PN: Catalase protects cardiomyocyte function in models of type 1 and type 2 diabetes. *Diabetes* 53:1336–1343, 2004
29. Sparagna GC, Hickson-Bick DL, Buja LM, McMillin JB: A metabolic role for mitochondria in palmitate-induced cardiac myocyte apoptosis. *Am J Physiol Heart Circ Physiol* 279:H2124–H2132, 2000
30. Listenberger LL, Ory DS, Schaffer JE: Palmitate-induced apoptosis can occur through a ceramide-independent pathway. *J Biol Chem* 276:14890–14895, 2001
31. Miller TA, LeBrasseur NK, Cote GM, Trucillo MP, Pimentel DR, Ido Y, Ruderman NB, Sawyer DB: Oleate prevents palmitate-induced cytotoxic stress in cardiac myocytes. *Biochem Biophys Res Commun* 336:309–315, 2005
32. Loskovich MV, Grivennikova VG, Cecchini G, Vinogradov AD: Inhibitory effect of palmitate on the mitochondrial NADH: ubiquinone oxidoreductase (complex I) as related to the active-de-active enzyme transition. *Biochem J* 387:677–683, 2005
33. Kawakami M, Okabe E: Superoxide anion radical-triggered Ca²⁺ release from cardiac sarcoplasmic reticulum through ryanodine receptor Ca²⁺ channel. *Mol Pharmacol* 53:497–503, 1998
34. Goldhaber JL, Qayyum MS: Oxygen free radicals and excitation-contraction coupling. *Antioxid Redox Signal* 2:55–64, 2000
35. Kaplan P, Babusikova E, Lehotsky J, Dobrota D: Free radical-induced protein modification and inhibition of Ca²⁺-ATPase of cardiac sarcoplasmic reticulum. *Mol Cell Biochem* 248:41–47, 2003
36. Buchanan J, Mazumder PK, Hu P, Chakrabarti G, Roberts MW, Yun UJ, Cooksey RC, Litwin SE, Abel ED: Reduced cardiac efficiency and altered substrate metabolism precedes the onset of hyperglycemia and contractile dysfunction in two mouse models of insulin resistance and obesity. *Endocrinology* 146:5341–5349, 2005
37. How OJ, Aasum E, Severson DL, Chan WY, Essop MF, Larsen TS: Increased myocardial oxygen consumption reduces cardiac efficiency in diabetic mice. *Diabetes* 55:466–473, 2006
38. Coort SL, Luiken JJ, van der Vusse GJ, Bonen A, Glatz JF: Increased FAT (fatty acid translocase)/CD36-mediated long-chain fatty acid uptake in cardiac myocytes from obese Zucker rats. *Biochem Soc Trans* 32:83–85, 2004
39. Zima AV, Kockskämper J, Mejia-Alvarez R, Blatter LA: Pyruvate modulates cardiac sarcoplasmic reticulum Ca²⁺ release in rats via mitochondria-dependent and -independent mechanisms. *J Physiol* 550:765–783, 2003
40. Carvajal K, Banos G, Moreno-Sanchez R: Impairment of glucose metabolism and energy transfer in the rat heart. *Mol Cell Biochem* 249:157–165, 2003
41. Xiang JZ, Kentish JC: Effects of inorganic phosphate and ADP on calcium handling by the sarcoplasmic reticulum in rat skinned cardiac muscles. *Cardiovasc Res* 29:391–400, 1995
42. Kockskämper J, Zima AV, Blatter LA: Modulation of sarcoplasmic reticulum Ca²⁺ release by glycolysis in cat atrial myocytes. *J Physiol* 564:697–714, 2005
43. Xu KY, Zweier JL, Becker LC: Functional coupling between glycolysis and sarcoplasmic reticulum Ca²⁺ transport. *Circ Res* 77:88–97, 1995
44. Hüser J, Wang YG, Sheehan KA, Cifuentes F, Lipsius SL, Blatter LA: Functional coupling between glycolysis and excitation-contraction coupling underlies alternans in cat heart cells. *J Physiol* 524:795–806, 2000
45. Diaz ME, O'Neill SC, Eisner DA: Sarcoplasmic reticulum calcium content fluctuation is the key to cardiac alternans. *Circ Res* 94:650–656, 2004